# Active Vibration Suppression of a Flexible Structure Using Sliding Mode Control

**Mehmet Itik**
*Erciyes University, Yozgat Engineering and Architecture Faculty, Mechanical Engineering Department, Yozgat, Turkey*
**Metin U. Salamci***
*Gazi University, Engineering and Architecture Faculty, Mechanical Engineering Department, 06570, Maltepe/Ankara, Turkey*

In this paper, sliding mode control (SMC) is designed and applied to an elastic structure to suppress some of its vibration modes. The system is an elastic beam clamped on one end and the designed controller uses only the deflection measurement of the free end. The infinite dimensional mathematical model of the beam is reduced to an ordinary differential equation set to represent the behavior of required modes. Since the states of the finite dimensional model are not physically measurable quantities, an observer is designed to estimate these states by measuring the tip deflection of the beam. The performance of the observer is important because the observed states are used in the SMC design. In this study, by using the output information, an observer is designed and tested to estimate the states of the finite dimensional model of the beam. Then the designed SMC is applied to the experimental beam system which gives satisfactory suppressed vibrations.

**Key Words :** Sliding Mode Control, Active Vibration Control, Observer Design, Elastic Structures

## 1. Introduction

Sliding Mode Control (SMC) for Linear Time Invariant (LTI) systems is well-defined and studied in details by many researchers (Dorling and Zinober, 1986; Spurgeon and Edwards, 1998; Utkin, 1992; Utkin and Yang, 1978; Young, 1993; Zinober, 1990). In general, SMC design procedure for LTI systems can be divided into two stages; sliding surface design where the system is restricted to remain on a linear hyper-plane in the state space and control synthesis which will drive the system to the designed surface. Sliding surface design for an LTI system is generally based on a linear coordinate transformation which splits the LTI system into two subsystems; one of which has control input and the other remains without control. While the subsystem with control input is controlled, the overall system is derived to the designed linear sliding surface. Once the system reaches to the sliding surface, its behavior is characterized by the hyper-plane. The parameters (slopes) of the sliding surface are determined so that the subsystem without control exhibits stable behavior.

SMC design for nonlinear systems is also studied by various mathematicians and engineers (Banks et al., 1999; DeCarlo et al., 1988; Utkin, 1992). Nevertheless there is no systematic method to be generalized to all types of nonlinear systems. This is because; it is not an easy job to find a coordinate transformation (either linear or non-

* Corresponding Author,
**E-mail** : msalamci@gazi.edu.tr
**TEL** : +90-312-2317400; **FAX** : +90-312-2319810
Gazi University, Engineering and Architecture Faculty, Mechanical Engineering Department, 06570, Maltepe/Ankara, Turkey. (Manuscript **Received** September 1, 2005; **Revised** May 29, 2006)

linear) which will split the nonlinear system into two subsystems like the one in LTI systems. Even though there exists such a coordinate system, there are many difficulties in finding the surface parameters resulting in stability for the subsystem having no control input. Although there are some suggested methods, sliding surface design for nonlinear systems is still an active research area (Salamci, 1999 ; Salamci et al., 2000).

SMC is applied to many physical system models including force and position control of robots, induction motor control, satellites and flexible structures (Choi and Kim, 2003 ; Young, 1993 ; Zinober, 1990). However there are still few reported experimental results in the literature. This is mainly due to its high frequency nature which makes the control signal production very difficult in the implementation. However, by the representation of high frequency actuators in the market, SMC becomes feasible in many engineering applications. For instance, piezoceramic actuators are now commonly used in the vibration control of flexible structures.

Active vibration suppression of flexible structures is an important engineering application since light structures are becoming main elements in the engineering systems. Therefore various control strategies have been suggested and applied to different flexible systems to suppress vibrations. Cavallo et al.(1999), Itik et al.(2005) and Young and Ozguner (1993) have applied SMC, LQG control has been suggested by Jeon et al.(2002) and by Petersen and Pota (2003), QFT Control has been applied by Choi et al.(1999), and $H_\infty$ control is studied by Dosch et al.(1995), Itik et al.(2005), Zames (1981) and Zames and Francis (1983). In these studies, infinite dimensional flexible structures are, in generally, modeled as finite dimensional linear systems by taking some of the vibration modes into consideration by means of the assumed mode method and Finite Element Model.

In this paper, we shall design and apply SMC to a clamped-free flexible beam in order to suppress the first two vibration modes. The partial differential equation (PDE) of the beam obtained from Euler-Bernoulli beam equation is transformed to finite dimensional ordinary differential equations (ODEs) by using the assumed mode method. As the SMC uses states of the system, which are not measurable, an observer is designed to estimate the states variables by measuring the tip point displacement of the beam by means of a laser displacement sensor. Since the control algorithm is based on state variables, the states of the system should be estimated in a short time which makes the observer design critical. The designed control algorithm is then applied to an experimental flexible beam system.

The organization of the paper is as follows ; in Section 2, the system modeling is described. Section 3 gives the controller and observer design. In section 4, simulation and experimental results are given. Finally, conclusions are given in Section 5.

## 2. The Beam Model

The flexible structure studied here is shown in Fig. 1. As shown, the elastic beam is clamped in one end and free on the other. Two piezoceramic patches (PZT-Lead-Zirconate-Titanate) are bonded to the flexible beam as actuators near the fixed end and a laser displacement sensor is used to measure tip point displacement.

The parameters of the flexible beam and PZT patches are given in Table 1. Compared to the beam length, $L$ (0.507 m), PZT length ($l_2-l_1=$ 0.05 m) is very small and similarly PZT thickness, $t_p$ ($6.1\times10^{-4}$ m) is small compared to beam thickness, $t_b$ (0.002 m). Therefore effect of elasticity due to PZT element in the system may be neglected in the derivation of mathematical expression of the model.

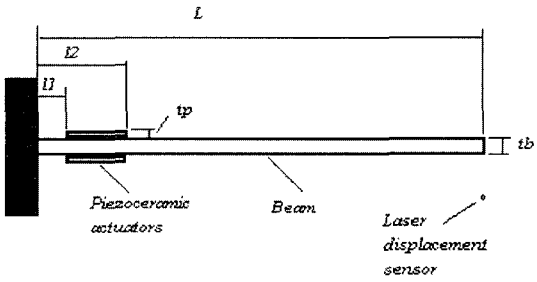


**Fig. 1** Flexible beam model

**Table 1** Parameters of flexible beam

| | |
|---|---|
| Beam length, $L$ | 0.507 m |
| Beam width, $b$ | 0.051 m |
| Beam thickness, $t_b$ | 0.002 m |
| Beam density, $\rho$ | 2480 kg/m$^3$ |
| Beam Young's modulus, $E$ | $70\times10^9$ N/m$^2$ |
| PZT position, $l_1$ | 0.026 m |
| PZT position, $l_2$ | 0.076 m |
| Charge constant, $d_{31}$ | $-200\times10^{-12}$ m/V |
| PZT Young's modulus, $E_p$ | $60\times10^9$ N/m$^2$ |
| PZT width, $w$ | 0.051 m |
| PZT thickness, $t_p$ | $6.1\times10^{-4}$ m |

Having considered uniform elastic beam structure, (i.e., density, cross-sectional area, moment of inertia and Young's module do not change much along the beam length), by using the well-known Euler-Bernoulli beam equation, the system can be described by the following PDE ;

$$\frac{\partial^2}{\partial x^2}\left[EI\frac{\partial^2 y(x,t)}{\partial x^2}\right]+\rho A\frac{\partial^2 y(x,t)}{\partial t^2}=C_a\frac{\partial^2 V_a(x,t)}{\partial t^2} \tag{1}$$

where $y(x,t)$ is the deflection along the $x$-axis, $E$ is the Young's modulus, $I$ is the moment of inertia, $A$ is the cross-sectional area, and $\rho$ is the density of the uniform beam. $V_a(x,t)$ is the applied control voltage to piezoceramic actuators. Since piezoceramic actuators are uniform along their lengths, the control voltage $V_a(x,t)$ can be replaced by $V_a(t)$. The constant $C_a$ is given by the following equation ;

$$C_a=E_p d_{31} b(t_b+t_p) \tag{2}$$

where $E_p$ is the Young's modulus, $t_p$ the thickness, and $d_{31}$ the electric charge constant of piezoceramic patches. $b$ and $t_b$ are the width and thickness of the beam respectively.

Euler-Bernoulli beam model is a distributed parameter model which is governed by PDE's having infinite number of dimensions. This makes it difficult to design and implement SMC algorithm. In order to simplify the design of SMC, Euler-Bernoulli beam equation is truncated to finite number of series by using assumed modes approach. By this approach, the deflection of the beam is given as functions of modal coordinates and mode shape functions as depicted in Eq. (3a). Then the following ODE's can be obtained.

$$y(x,t)=\sum_{i=1}^{\infty} q_i(t)\,\phi_i(x) \tag{3a}$$

$$\ddot{q}_i(t)+2\xi_i w_i\dot{q}_i(t)+w_i^2 q_i(t)=\frac{C_a}{\rho AL^3}[\phi_i'(l_1)-\phi_i(l_2)]\,V_a(t) \quad \text{for } i=1,\cdots,\infty \tag{3b}$$

where $q_i(t)$, $\phi_i(x)$, $\phi_i'(x)$, $w_i$, $\xi_i$ are the $i$-th modal co-ordinate, mode shape function, modal slope of the beam, natural frequency, and damping ratio respectively. In this study, the SMC is designed to suppress the first two vibration modes of the beam ($i=1, 2$). The mode shape function for clamped-free beam is given by

$$\phi_i(x)=L(\cosh(\lambda_i x)-\cos(\lambda_i x))-k_i(\sinh(\lambda_i x)-\sin(\lambda_i x)) \tag{4}$$

where the constant $k_i$ is given by ;

$$k_i=\frac{\cosh(\lambda_i L)+\cos(\lambda_i L)}{\sinh(\lambda_i L)+\sin(\lambda_i L)} \tag{5}$$

The quantities $\lambda_i$ are the real roots of $\cos(\lambda_i L)\cos(\lambda_i L)=-1$. For the first two modes of the beam, the quantities are calculated as $\lambda_i=3.7955$ and $\lambda_2=9.5020$. The natural frequencies can be computed from

$$w_i=\sqrt{\frac{EI}{\rho A}}\lambda_i^2 \tag{6}$$

where $I=bt_b^3/12$, $A=bt_b$. The natural frequencies are calculated as $w_1=6.5720$ and $w_2=41.1890$ Hz. Damping ratios of the first two modes of the flexible beam are obtained as $\xi_i=0.07$ and $\xi_2=0.02$ (Petersen and Pota, 2003). By using the calculated values for the flexible beam, the frequency response of the unforced system for the first two modes is plotted in Fig. 2.

The second order ODE set given by Eq. (3b) can be described in the state space form. For the first two modes (i.e., $i=1, 2$), the beam model given in Eq. (3b) is written as follows ;

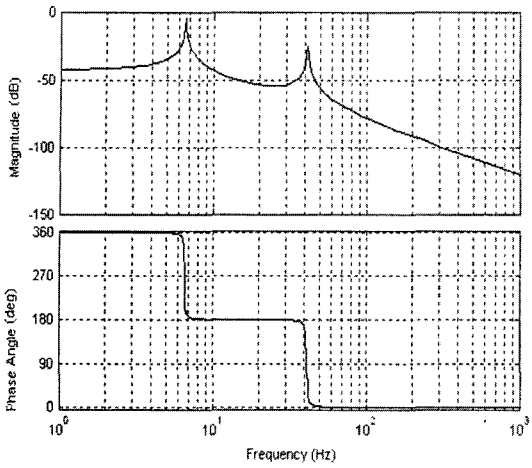


**Fig. 2** Frequency response of the elastic beam

$$\dot{x}(t)=\begin{bmatrix}0 & 1 & 0 & 0\\ -w_1^2 & -2\xi_1 w_1 & 0 & 0\\ 0 & 0 & 0 & 1\\ 0 & 0 & -w_2^2 & -2\xi_2 w_2\end{bmatrix}x(t)+\frac{C_a}{\rho AL^3}\begin{bmatrix}0\\ \phi_1'(l_1)-\phi_1'(l_2)\\ 0\\ \phi_2'(l_1)-\phi_2'(l_2)\end{bmatrix}u(t) \tag{7}$$

where $x(t)=[q_1\ \dot{q}_1\ q_2\ \dot{q}_2]^T$. Note that the state variables are the modal coordinates and their first derivatives which are not measurable.

## 3. SMC Design

SMC design procedure is generally divided into two stages; (1) design of sliding surface on which the system will have stable motion and (2) synthesis of the control algorithm such that the trajectories of the closed loop motion are directed to the designed sliding surface. In both stages, the system states are necessary to complete the implementation. Since the states of the flexible beam system can not be measured directly, in this study an observer is designed to obtain the system states by measuring the tip point displacement of the beam. These design stages are summarized below for the sake of completeness.

### 3.1 Sliding surface and controller design

SMC design procedure for general LTI systems is well defined (see Utkin, (1992) and the references therein) and is summarized here. For an LTI system represented by

$$\begin{aligned}\dot{x}(t)&=Ax(t)+Bu(t)\\ y(t)&=Cx(t)\end{aligned} \tag{8}$$

where $x\in R^n$, $u\in R^m$, $y\in R^p$, $A\in R^{nxn}$ and $B\in R^{nxm}$. The pair $(A, B, C)$ is to be fully controllable and observable. Sliding surface for the system given by Eq. (8) is now;

$$\sigma(x,t)=Sx(t) \tag{9}$$

where $S\in R^{m\times n}$ is the sliding surface matrix and it represents the slope of the sliding surface. This matrix is selected in order to satisfy a stable motion for the closed loop system. To simplify the selection of sliding surface slope, the system given by Eq. (8) is defined in another coordinate system by using a linear transformation $z=Tx$. The transformation matrix $T\in R^{nxn}$ is selected so that $\tilde{B}=T^{-1}B=[[0]\ \vdots\ [B_2]]^T$ which splits the system into two subsystems; one without control ($z_1\in R^{n-m}$) and the other with control ($z_2\in R^m$). In the new coordinate system, the system matrix becomes;

$$\tilde{A}=T^{-1}AT=\begin{bmatrix}\tilde{A}_{11} & \tilde{A}_{12}\\ \tilde{A}_{21} & \tilde{A}_{22}\end{bmatrix} \tag{10}$$

Similarly, the system in the new coordinate system can be represented as follows;

$$\begin{aligned}\dot{z}_1(t)&=\tilde{A}_{11}z_1(t)+\tilde{A}_{12}z_2(t)\\ \dot{z}(t)&=\tilde{A}_{21}z_1(t)+\tilde{A}_{22}z_2(t)+B_2u\end{aligned} \tag{11}$$

where $z_1\in R^{n-m}$, $z_2\in R^m$. The sliding surface, on the other hand, can be written in the new coordinates as

$$\sigma(z,t)=z_2(t)+\tilde{S}_1z_1(t) \tag{12}$$

where $\tilde{S}_1\in R^{(n-m)\times(n-m)}$ and satisfies $\tilde{S}=\lfloor[I]\ \vdots\ \lfloor\tilde{S}_1\rfloor\rfloor=ST^{-1}$. On the sliding surface $\sigma(z,t)=0$, which implies $z_2(t)=-\tilde{S}_1z_1(t)$. This equation is like a state feedback control for the $z_1\in R^{n-m}$ subsystem. In order to obtain a stable sliding surface, the $z_1\in R^{n-m}$ subsystem must have stable dynamics. Therefore $\tilde{S}_1$ are chosen so that the eigenvalues of $(A_{11}-A_{12}\tilde{S}_1)$ matrix have negative real parts.

For the controller design stage, the control input is designed such that the system trajectories reach the sliding surface (reaching phase) and then are stayed (sliding phase) on the sliding surface. This is guaranteed by satisfying the following inequality (note that the same condition can be expressed by different equations);

$$\begin{aligned} &\dot{\sigma}(x,t)>0 \text{ if } \sigma(x,t)<0 \\ &\dot{\sigma}(x,t)<0 \text{ if } \sigma(x,t)>0 \end{aligned} \tag{13}$$

The control law is selected in order to satisfy Eq. (13) and it is given by;

$$u(t)=u_{eq}(t)+u_n(t) \tag{14}$$

where $u_{eq}(t)=-(\tilde{S}\tilde{B})^{-1}\tilde{S}\tilde{A}z(t)$ and $u_n(t)=-Ksign(\sigma)$. The constant $K$ is a positive number and determines the reaching time to the sliding surface.

### 3.2 Observer design

As the modal co-ordinate and modal velocity can not be measured directly, an observer is designed in this work to estimate the system states. The observer is a Luenberger observer for linear systems given by;

$$\dot{\hat{x}}(t)=A\hat{x}(t)+Bu(t)+L(y-C\hat{x}(t)) \tag{15}$$

where $\hat{x}\in R^n$ dimensional estimated states. Note that the system should be observable to estimate the states. By defining $e=x-\hat{x}$ as the error between real and estimated states, the error dynamics of the observed system can be written as follows;

$$\dot{e}(t)=(A-LC)e(t) \tag{16}$$

Therefore observer gain matrix, $L$, is chosen such that $(A-LC)$ matrix has negative eigenvalues which implies that error dynamics is stable and the estimated states converges to the exact values. However, stability of the error dynamics is not the only criteria in the selection of the observer gain matrix. The observer should be quick enough to estimate the states as these states are used in the SMC design.

## 4. Simulation and Experimental Results

The designed SMC algorithm is first simulated by using the model of the flexible beam. The model includes the first two vibration modes of the system. By using the numerical values of the model, the system can be described by the following ODE's.

$$\dot{x}=Ax+Bu \tag{17a}$$

$$y=Cx \tag{17b}$$

where

$$A=\begin{bmatrix} 0 & 1 & 0 & 0 \\ -1705{,}14 & -0{,}578_1 & 0 & 0 \\ 0 & 0 & 0 & 1 \\ 0 & 0 & -66976{,}58 & -3{,}623 \end{bmatrix},$$

$B=[0\ 0.14\ 0\ 0.52]^T$ and $C=[0{,}9879\ 0\ -0{,}9879\ 0]$

Since $rank([B : AB : A^2B : A^2B])=4$ and $rank([C : AC : A^2C : A^3C])=4$, the system model is controllable and observable. By using the following non-singular coordinate transformation matrix, $z=Tx$, the system is described by Eq. (18).

$$T=\begin{bmatrix} 1 & 0{,}52 & 4 & -0{,}14 \\ 2 & 0{,}52 & 1 & -0{,}14 \\ 1 & 1{,}04 & 2 & -0{,}28 \\ 4 & 1 & 2 & -0{,}25 \end{bmatrix}$$

$$\dot{z}=\tilde{A}z+\tilde{B}u \tag{18a}$$

$$y=\tilde{C}z \tag{18b}$$

where

$$\tilde{A}=10^5\begin{bmatrix} 3{,}1095 & -1{,}6925 & -0{,}7087 & 0{,}0244 \\ 3{,}1104 & -1{,}6890 & -0{,}7109 & 0{,}0230 \\ 6{,}2211 & -3{,}3770 & -1{,}4225 & 0{,}0455 \\ 0{,}0545 & 0{,}0348 & -0{,}0099 & 0{,}0020 \end{bmatrix},$$

$\tilde{B}=[0\ 0\ 0\ 1]^T$ and $C=[-0{,}3293\ 0.7684\ -0{,}2195\ 0]$

As described in section 3, a Luenberger observer is designed to estimate the state variables by measuring the tip point deflection of the beam. The observer gain is important in the estimation

procedure and it should be selected not only to satisfy stable observer dynamics but also to yield quick estimation of the states. In order to show the effect of observer gain matrix, $L$, two simulation results are given in Fig. 4 and Fig. 5 for different observer gain matrices. Fig. 3 shows the free vibration response of the beam model for a 0.04 m initial tip deflection. In the simulations, observers are designed in order to estimate the tip point deflection of the beam. Fig. 4 gives the observer performance for the gain matrix of $L_1=10^6[-0{,}956\ -0{,}9559\ -1{,}9118\ 0{,}0171]^T$. Fig. 5, on the other hand, plots the observer and system responses for the gain matrix of $L_2=10^5[5{,}374\ 5{,}381\ 10{,}758\ 0{,}105]^T$.

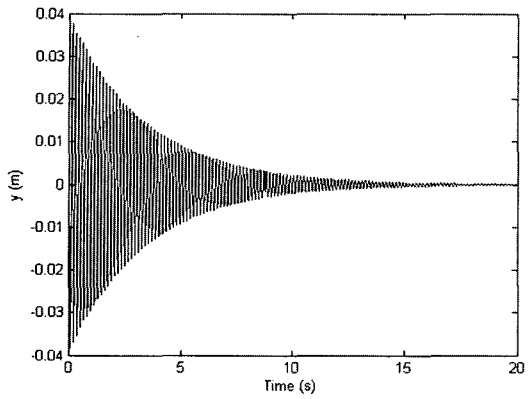


**Fig. 3** Free response of the beam model for 0.04 m initial tip deflection

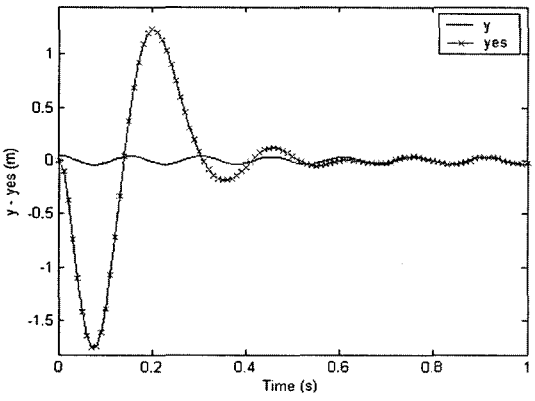


**Fig. 4** Beam model and observer responses for $L_1$

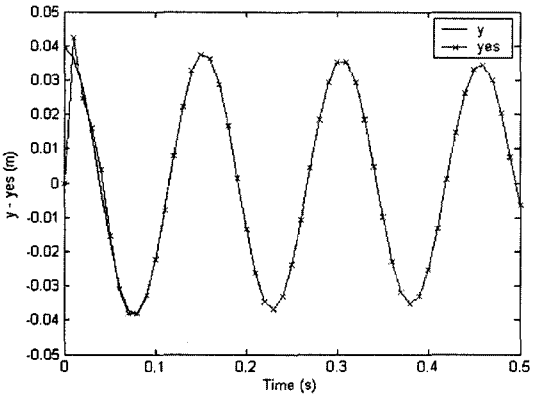


**Fig. 5** Beam model and observer responses for $L_2$

Although two gain matrices give stable error dynamics for the observer (both observers estimate the states), the second gain matrix results in very quick estimation of the state variables. As seen in Fig. 5, the observer estimates the tip point deflection of the beam accurately less than 0.1 sec and the overshoots are negligible. This is very important in the implementation of SMC because the control law uses the estimated state variables. Slow estimation of state variables results in high control voltages and may cause system instability.

By using the estimated state variables, the sliding surface and SMC can be designed as outlined in section 3. The sliding surface is now;

$$\sigma(z)=z_2+[-0.5361\ -2.0695\ 1.2935]z_1$$

By this sliding surface, $z_1\in R^3$ subsystem will have the following eigenvalues on the surface.

$$\lambda_{1,2}=-5\pm 175j\,;\ \lambda_3=-20$$

The equivalent part of the SMC in Eq. (14) is determined to be;

$$u_{eq}=[254.9466\ 19.8558\ -137.1589\ -25.7987]z$$

And the total control is now;

$$u(t)=u_{eq}(t)+u_n(t) \qquad (19)$$

where $u(t)=-0.5sign(\sigma(z))$. By applying control law given in Eq. (19), the control signal history is obtained as given by Fig. 6. From Fig. 6, it is seen that the control signal is between $\pm 200$V. However the PZT patches work between $\pm 150$V. In order to see the effect of bounded control signal on the system performance, we have

bounded the designed SMC between and applied this control to the system model. The bounded control signal is given in Fig. 7. Fig. 8 shows the system response to the bounded SMC and sliding surface variation is plotted in Fig. 9. Since the required control voltages do not exceed limitations much, the system responses to the bounded SMC is satisfactory and the vibrations are suppressed in a short time. As seen in Fig. 9, the sliding surface is reached in less than 0.5 sec and the system remains on the surface afterwards even the bounded control input is applied.

After the simulation studies, we shall apply SMC to an experimental beam system. The experimental setup used in this study is shown in Fig. 10. Fig. 11 gives the schematic diagram of the experimental setup of the flexible beam system. In the experimental setup $507\times51\times2$ mm aluminum beam and $20\times25\times0.61$ mm dimensional 8 pieces BM500 type piezoelectric (PZT, Lead-Zirconate-Titanate) patches were used. The maximum working frequency of the PZT elements is 500 Hz

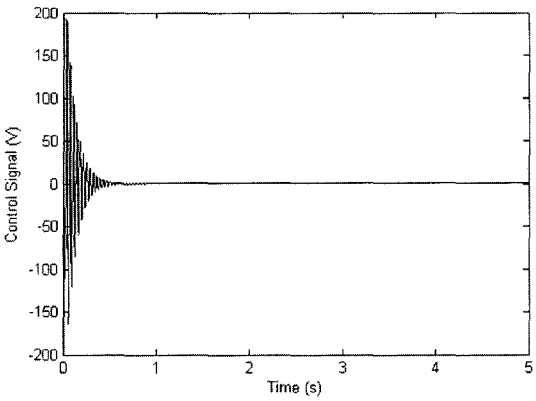


**Fig. 6** Control voltage to PZT patches

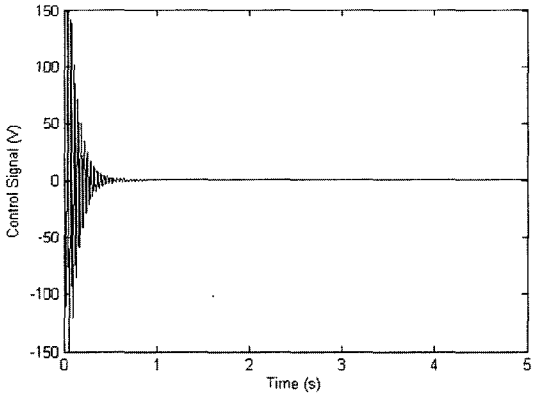


**Fig. 7** Bounded control signal

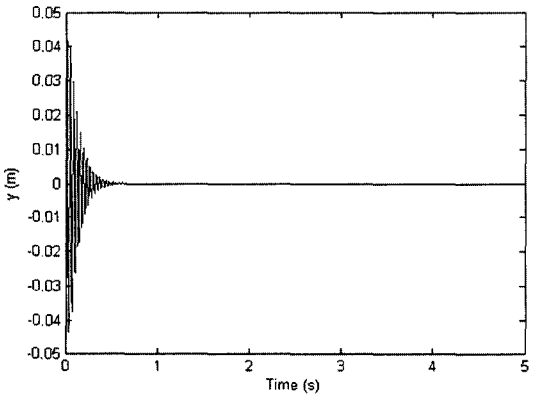


**Fig. 8** Closed loop response of the beam model to the bounded SMC

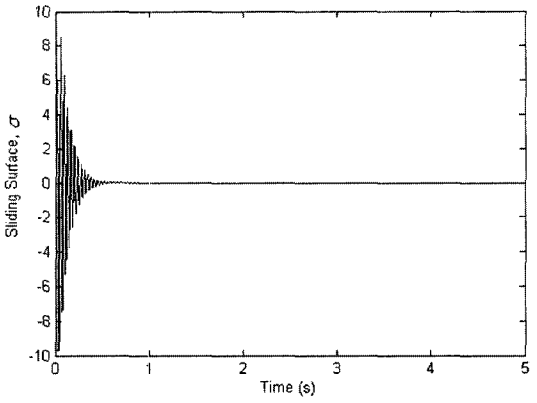


**Fig. 9** Sliding surface for bounded control

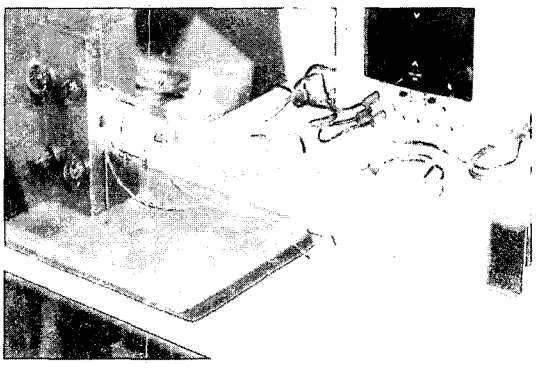

**Fig. 10** The flexible beam system

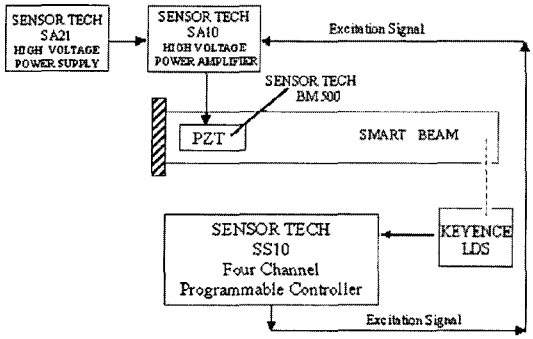


**Fig. 11** Experimental setup of the flexible beam system

which makes the designed SMC algorithm applicable to the system.

In order to implement the controller designed in section 3, Sensortech SS10 type four-channel programmable controller and data acquisition system was used. This programmable controller system is controlled by a personal computer which runs with Linux operating system. A program was written in C programming language in order to implement SMC algorithm to four-channel programmable controller system. Then the control signal was send to Sensortech SA10 high voltage power amplifier in order to apply to PZT patches. The controller system can send signal between $-10$V and $+10$V, then this signal was amplified 15 times by high voltage power amplifier. Tip point displacement of the beam was measured by Keyence laser displacement sensor and the measured signal was fed back to controller system. The sampling frequency of the laser displacement sensor is 1024 $\mu$s.

The open loop time response of the beam for 0.04 m initial tip point displacement and zero velocity is given in Fig. 12. The SMC was applied to the beam and controlled time response of the beam is given in Fig. 13 for the same initial conditions. Applied control input to PZT patches is given in Fig. 14.

From Fig. 13, it is seen that the applied SMC can successfully suppress the vibrations in the flexible beam system. Although the first two vibration modes have been suppressed by the designed SMC algorithm in this study, it is always possible to extend the approach to the higher vibration modes.

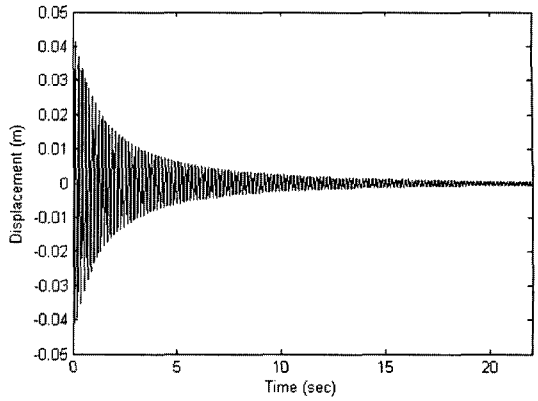


**Fig. 12** Free response of the beam for 0.04 m tip point displacement

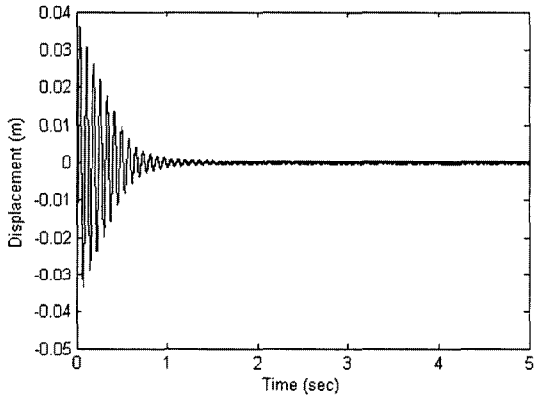


**Fig. 13** Closed loop response of the beam for 0.04 m tip point displacement

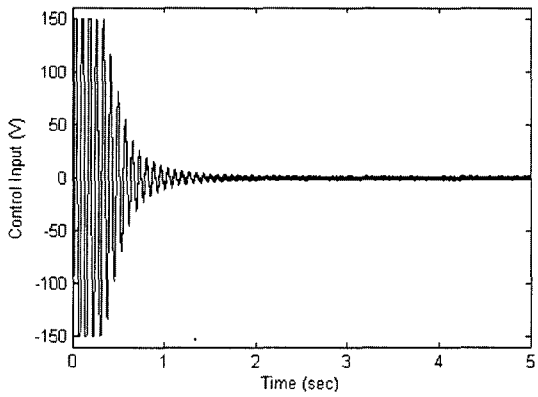


**Fig. 14** Applied control voltage to PZT patches

## 5. Conclusions

In this work, SMC has been designed and applied to a flexible beam system to suppress the first two vibration modes. In the SMC design, only output information was used and the state variables, which are necessary to construct SMC, were estimated by using a Luenberger observer. The observer gain matrix was selected such that both the stability of observer and fast estimation of the states were guaranteed. From the experimental results, it is seen that the designed controller exhibits satisfactory performance and suppresses the vibration of the beam. The approach can be extended to the suppression of higher vibration modes. In that case, higher dimensional system models should be used.

## Acknowledgments

The authors thank Prof. Dr. Yavuz Yaman and Mrs. F. Demet Ulker from the Middle East Technical University for their help in using the experimental setup.

## References

Bailey, T. and Hubbard, J. E., 1985, "Distributed Piezoelectric-Polymer Active Vibration Control of a Cantilever Beam," *Journal of Guidance, Control and Dynamics*, Vol. 8, No. 5, pp. 605~611.

Banks, S. P., Salamci, M. U. and Ozgoren, M. K., 1999, "On the Global Stabilization of Nonlinear Systems via Switching Manifolds," *Turkish Journal of Electrical Engineering & Computer, Elektrik*, Vol. 7, No. 1-3, pp. 1~17.

Cavallo, A., De Maria, G. and Setola, R., 1999, "A Stable Manifold Approach for Vibration Reduction of Flexible Systems," *Automatica*, Vol. 35, pp. 1689~1696.

Choi, J. J. and Kim, J. S., 2003, "Robust Control for Rotational Inverted Pendulums Using Output Feedback Sliding Mode Controller and Disturbance Observer," *KSME International Journal*, Vol. 17, No. 10, pp. 1466~1474.

Choi, S. B., Cho, S. S. and Park, Y. P., 1999, "Vibration and Position Tracking Control of Piezoceramic-Based Smart Structures via QFT," *Journal of Dynamic Systems, Measurement and Control*, Vol. 121, pp. 27~33.

DeCarlo, R. A., Zak, S. H. and Matthews, G. P., 1988, "Variable Structure Control of Nonlinear Multivariable Systems: A Tutorial," *Proceeding of IEEE*, Vol. 76, No. 3, pp. 212~232.

Dorling, C. M. and Zinober, A. S. I., 1986, "Two Approaches to Hyperplane Design in Multivariable Structure Control Systems," *International Journal of Control*, Vol. 44, pp. 65~82.

Dosch, J., Leo, D. and Inmann, J., 1995, "Modeling and Control for Vibration Suppression of a Flexible Active Structure," *Journal of Guidance, Control and Dynamics*, Vol. 18, pp. 340~346.

Itik, M., Salamci, M. U., Ulker, F. D. and Yaman, Y., 2005, "Active Vibration Suppression of a Flexible Beam via Sliding Mode and H-infinity Control," to be presented in *IEEE Conference on Decision and Control and European Control Conference (CDC-ECC'05)* to be held in Seville, Spain, on December 12-15.

Jeon, S., Ahn, H. J. and Han, D. C., 2002, "Model Validation and Controller Design for Vibration Suppression of Flexible Rotor Using AMB," *KSME International Journal*, Vol. 16, No. 12, pp. 1583~1593.

Petersen, I. R. and Pota H. R., 2003, "Minimax LQG Optimal Control of a Flexible System," *Control Engineering Practice*, Vol. 11, pp. 1273~1287.

Salamci, M. U., 1999, "Two New Switching Surface Design Techniques for Nonlinear Systems with Their Applications to Missile Control," PhD. Thesis, Middle East Technical University.

Salamci, M. U., Ozgoren, M. K. and Banks, S. P., 2000, "Sliding Mode Control with Optimal Sliding Surfaces for a Missile Autopilot Design," *AIAA Journal of Guidance, Control and Dynamics*, Vol. 23, No. 4, pp. 719~727.

Shin, H. C. and Choi, S. B., 2001, "Position Control of Two Link Flexible Manipulator Featuring Piezoelectric Actuators and Sensors," *Mechatronics*, Vol. 11, pp. 707~729.

Spurgeon, S. K. and Edwards, C., 1998, "Sliding Mode Control: Theory and Applications," Taylor & Francis, London.

Utkin, V. I. and Yang, K. D., 1978, "Methods for Constructing Discontinuity Planes in Multidimensional Variable Structure Systems," *Automation and Remote Control*, Vol. 39, pp. 1466~1470.

Utkin, V. I., 1992, "Sliding Modes in Control and Optimization," Springer Verlag, Berlin.

Young, K. K. D., (editor), 1993, "Variable Structure Control for Robotics and Aerospace Applications," Elsevier, Amsterdam.

Young, K. K. D. and Ozguner, U., 1993, "Frequency Shaping Compensator Design for Sliding Mode," *International Journal of Control*, Vol. 57, No. 5, pp. 1005~1019.

Zames, G. and Francis, B.A., 1983, "Feedback Minimax Sensitivity and Optimal Robustness," *IEEE Trans. On Automatic Control*, Vol. AC-28, No. 5, pp. 585~600.

Zames, G., 1981, "Feedback and Optimal Sensitivity: Model Reference Transformations, Multiplicative Seminorms, and Approximate Inverses," *IEEE Trans. On Automatic Control*, Vol. AC-26, No. 2, pp. 301~320.

Zinober, A. S. I., (editor), 1990, "Deterministic Control of Uncertain Systems," Peter Peregrinus Ltd., London.